

ORIGINAL ARTICLE

Early onset horizontal gaze palsy and progressive scoliosis due to a noncanonical splicing-site variant and a missense variant in the *ROBO3* gene

Sheng Yi^{1,2}  | Zailong Qin^{1,2}  | Xunzhao Zhou^{1,2} | Junjie Chen³ | Shang Yi^{1,2} | Qiuli Chen^{1,2} | Limei Huang^{1,2} | Qinle Zhang^{1,2} | Biyan Chen^{1,2} | Jingsi Luo^{1,2}

¹Genetic and Metabolic Central Laboratory, Guangxi Birth Defects Research and Prevention Institute, Maternal and Child Health Hospital of Guangxi Zhuang Autonomous Region, Nanning, China

²Guangxi Clinical Research Center for Pediatric Diseases, Guangxi Key Laboratory of Reproductive Health and Birth Defects Prevention, Guangxi Key Laboratory of Precision Medicine for Genetic Diseases, Guangxi Key Laboratory of Birth Defects and Stem Cell Biobank, Guangxi Key Laboratory of Birth Defects Research and Prevention, Maternal and Child Health Hospital of Guangxi Zhuang Autonomous Region, Nanning, China

³Department of Radiology, Maternal and Child Health Hospital of Guangxi Zhuang Autonomous Region, Nanning, China

Correspondence

Jingsi Luo and Biyan Chen, Laboratory of Genetics and Metabolism, Maternal and Child Health Hospital of Guangxi Zhuang Autonomous Region, Nanning 530003, People's Republic of China.
Email: ljs0815freedom@163.com and 1219557629@qq.com

Funding information

Guangxi Key Research and Development Program, Grant/Award Number: GuikeAB17195004; Health Department of Guangxi Zhuang Autonomous Region, Grant/Award Number: Z20200678; the Projects of Yu-Miao, Grant/Award Number: GXWCH-YMJH-2017006

Abstract

Background: Homozygous or compound heterozygous *ROBO3* gene mutations cause horizontal gaze palsy with progressive scoliosis (HGPPS). This is an autosomal recessive disorder that is characterized by congenital absence or severe restriction of horizontal gaze and progressive scoliosis. To date, almost 100 patients with HGPPS have been reported and 55 *ROBO3* mutations have been identified.

Methods: We described an HGPPS patient and performed whole-exome sequencing (WES) to identify the causative gene.

Results: We identified a missense variant and a splice-site variant in the *ROBO3* gene in the proband. Sanger sequencing of cDNA revealed the presence of an aberrant transcript with retention of 700 bp from intron 17, which was caused by a variation in the noncanonical splicing site. We identified five additional *ROBO3* variants, which were likely pathogenic, and estimated the overall allele frequency in the southern Chinese population to be 9.44×10^{-4} , by a review of our in-house database.

Conclusion: This study has broadened the mutation spectrum of the *ROBO3* gene and has expanded our knowledge of variants in noncanonical splicing sites. The results could help to provide more accurate genetic counseling to affected families and prospective couples. We suggest that the *ROBO3* gene should be included in the local screening strategy.

KEYWORDS

allele frequency, HGPPS, noncanonical splicing site, *ROBO3*, screening strategy

This is an open access article under the terms of the [Creative Commons Attribution-NonCommercial-NoDerivs](https://creativecommons.org/licenses/by-nc-nd/4.0/) License, which permits use and distribution in any medium, provided the original work is properly cited, the use is non-commercial and no modifications or adaptations are made.

© 2023 The Authors. *Molecular Genetics & Genomic Medicine* published by Wiley Periodicals LLC.

1 | INTRODUCTION

Horizontal gaze palsy with progressive scoliosis (HGPPS, MIM#607313) is an autosomal recessive disorder that is characterized by congenital absence or severe restriction of horizontal gaze and childhood-onset progressive scoliosis (Sharpe et al., 1975). This syndrome includes a distinctive brain stem malformation and crossing of certain brain stem neuronal pathways. The *ROBO3* gene (roundabout guidance receptor 3, MIM#608630) is necessary for hindbrain axon pathway crossing and morphogenesis (Jen et al., 2004). It contains 28 coding exons that encode a protein of 1386 amino acids, which make up five immunoglobulin (Ig)-like loops, three fibronectin (Fn) type III repeats, a transmembrane segment, and three conserved signaling motifs (CC0, CC2, and CC3) (Jen et al., 2004). Mutations in the *ROBO3* gene are responsible for HGPPS.

To date, almost 100 HGPPS patients have been identified, from different regions of the world. The vast majority of patients are family clustering cases and most of them were born from consanguineous parents (Xiu et al., 2021). Fifty-five different mutations have been found in the coding region of the *ROBO3* gene (Table S1). These included 23 missense mutations, 11 nonsense mutations, five splicing mutations, 15 frameshift mutations, and one in-frame deletion. This study presents a patient with HGPPS, from a nonconsanguineous Chinese family, with compound heterozygous variants in the *ROBO3* gene. This is the first report of HGPPS caused by a substitution in the non-canonical splicing site of the *ROBO3* gene.

In addition to the two novel variants observed in our patient, we identified a further five novel, likely pathogenic variants in the *ROBO3* gene by screening all variants in our in-house database. The expanded mutation spectrum of the *ROBO3* gene will improve the diagnosis of HGPPS. We calculated the total allele frequency (AF) of the pathogenic and likely pathogenic *ROBO3* variants. The data led us to speculate that some patients with HGPPS will not have obtained a definitive diagnosis, as the overall AF in our cohort was estimated to be almost 1/1000.

2 | PATIENT AND METHODS

2.1 | Patients and ethics approval

A total of 6886 participants (2313 patients and 4573 controls) were enrolled from January, 2016 to July, 2022 in the Maternal and Child Health Hospital of Guangxi Zhuang Autonomous Region. The patients involved were suffering from unrelated diseases, which included hematopathy (1425), endocrine abnormalities (221), immunologic abnormalities (59), hearing disorders (118), infertility (340), and

repeated miscarriage (150). The study was approved by the ethics committee of our hospital. Written informed consent was obtained from parents or guardians of all patients.

2.2 | DNA extraction and WES analysis

Peripheral blood samples from patients and their families were collected in vacutainer tubes containing anticoagulant ethylenediaminetetraacetic acid (EDTA). Genomic DNA was extracted with Lab-Aid DNA kit (Zeesan Biotech Co., Ltd, Xiamen, China) using standard procedures. Exome capture was performed using the Agilent SureSelect Human All Exon v6 kit (Agilent Technologies, Santa Clara, CA). The prepared DNA libraries were then sequenced on a HiSeq2500 platform (Illumina, San Diego, CA). Sequencing reads were aligned to the human reference genome (NCBI build GRCh37/hg19) using Burrows-Wheeler Aligner (BWA), and variant calling were performed with the Genome Analysis Toolkit (GATK). Copy number variants (CNVs) analysis using WES data were conducted by an in-house pipeline. Single-nucleotide variants (SNVs) and insertion-deletions (indels) were prioritized by TGex software (LifeMap Sciences, Alameda, CA). The genetic variant interpretation and criteria used to establish variant pathogenicity were determined according to the American College of Medical Genetics and Genomics (ACMG) and the Association for Molecular Pathology (AMP) guidelines (Richards et al., 2015).

2.3 | Sanger sequencing verification

The potential candidate variants were validated in patients and all available family members through Sanger sequencing. Specific PCR primers were used for the amplification of mutation sites and their flanking regions. The PCR amplifications were conducted using Premix LA Taq DNA Polymerase (Takara Biotechnology, Dalian, China). Purified PCR products were sequenced on an ABI 3130 genetic analyzer (Applied Biosystems, CA, USA).

2.4 | In silico analysis

To predict the potential effect of the novel missense variations, in silico analyses were performed using Mutation Taster (<http://www.mutationtaster.org>), SIFT (<http://sift.jcvi.org/>), PROVEAN (<http://www.provean.jcvi.org/>), and PolyPhen 2.0 (<http://genetics.bwh.harvard.edu/pph2/>). To assess the prediction of the effects of variants on splicing, varSEAK (<https://varseak.bio/>) was used as an in silico predictor.

2.5 | RNA extraction and cDNA sequencing

Fresh peripheral blood samples were collected into EDTA anticoagulation tubes. Total RNA was extracted using TRIzol reagent (Invitrogen, CA, USA) according to the manufacturer's instructions. After being quantified with agarose gel electrophoresis and NanoDrop ND-2000 (Thermo Fisher Scientific, MA, USA), 1 µg of mRNA was reverse-transcribed into cDNA using a First-strand cDNA Synthesis Kit (Takara Biotechnology, Dalian, China). The cDNA amplifications were carried out using the LA Taq polymerase (Takara Biotechnology, Dalian, China). The primer sequences were as follows: Forward primer: 5' AGTGCCCCAGTGCTGGTG 3' and reverse primer: 5' GAATCTGCCAGCCATGAGTAG 3'. The obtained PCR products were analyzed on a 1.5% agarose gel and directly sequenced on an ABI 3130 genetic analyzer (Applied Biosystems) after purification.

3 | RESULTS

3.1 | Clinical findings

The proband was a 16-year-old Chinese boy who was the first child to be born to healthy, nonconsanguineous parents (Figure 1a). The boy was born at full term by vaginal delivery with normal birth parameters (weight = 3.25 kg, height = 51 cm), after an uneventful pregnancy. There was no history of peri- or postnatal trauma or any other obvious infections. However, esotropia and restrictive ocular motility were noted shortly after birth. Neither eye could adduct or abduct but his vertical gaze was intact (Figure 1b). A further ophthalmologic examination showed normal

vision in both eyes, a normal optic fundus, and no visual field defect. Scoliosis was noted as the proband began turning over at 5 months and to sit at 7 months. The boy's speech was delayed by 18 months and he did not start to walk until 30 months. The child underwent surgery at 3 years of age to correct his esotropia. When he was 8 years old, thoracic and lumbar spine X-rays indicated thoracic scoliosis, with convexity toward the right, and the ribs on either side of the T12 thoracic vertebra were noticeably shorter (Figure 1c,d). His mental milestones were normal. According to his father, the boy had a sister (Figure 1a, II2) who had exhibited a congenital deficit of ocular motility in both eyes. Tragically, the girl died suddenly at the age of 5 months, following an infection.

3.2 | Genetic analysis

Using exome sequencing of the proband, a total of 821 variants were identified in coding regions and splice sites, after filtering out minor allele frequencies (MAF) of >0.01 from our local and publicly available databases. After clinical phenotype analysis, we identified compound heterozygous variants, c.437G>A (p.Arg146His) and c.2779+5G>C, in the *ROBO3* gene (NM_022370.4) of the proband. The variants were verified by Sanger sequencing and both asymptomatic parents were heterozygous carriers (Figure 2a). The maternally inherited missense variant was listed in the dbSNP database (rs768751790), but it has not been described in patients. The paternally inherited splice-site variant is novel, and aberrant splicing was verified by reverse transcription-PCR (RT-PCR) analysis on total RNA isolated from whole blood from the patient (Figure 2b). Both variants can be classified as likely pathogenic, following the ACMG/AMP guidelines (Table S2).

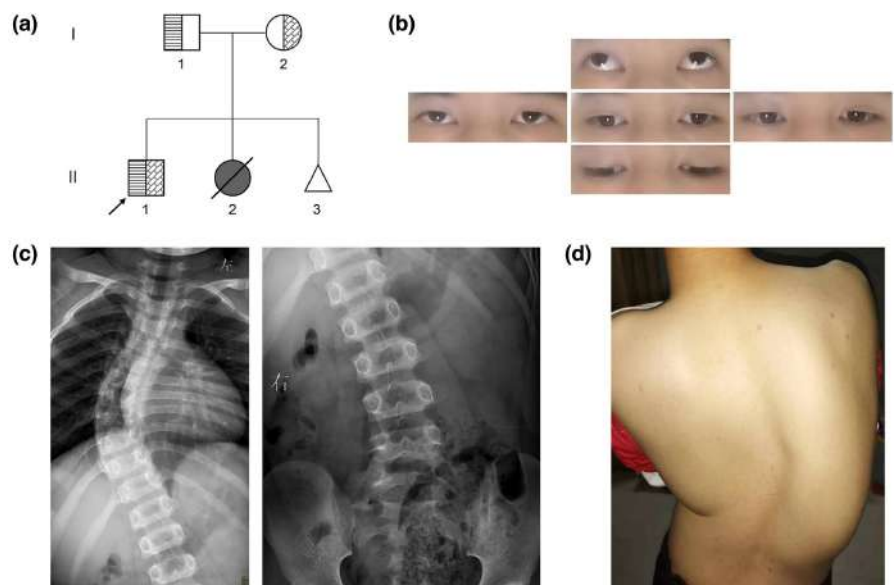
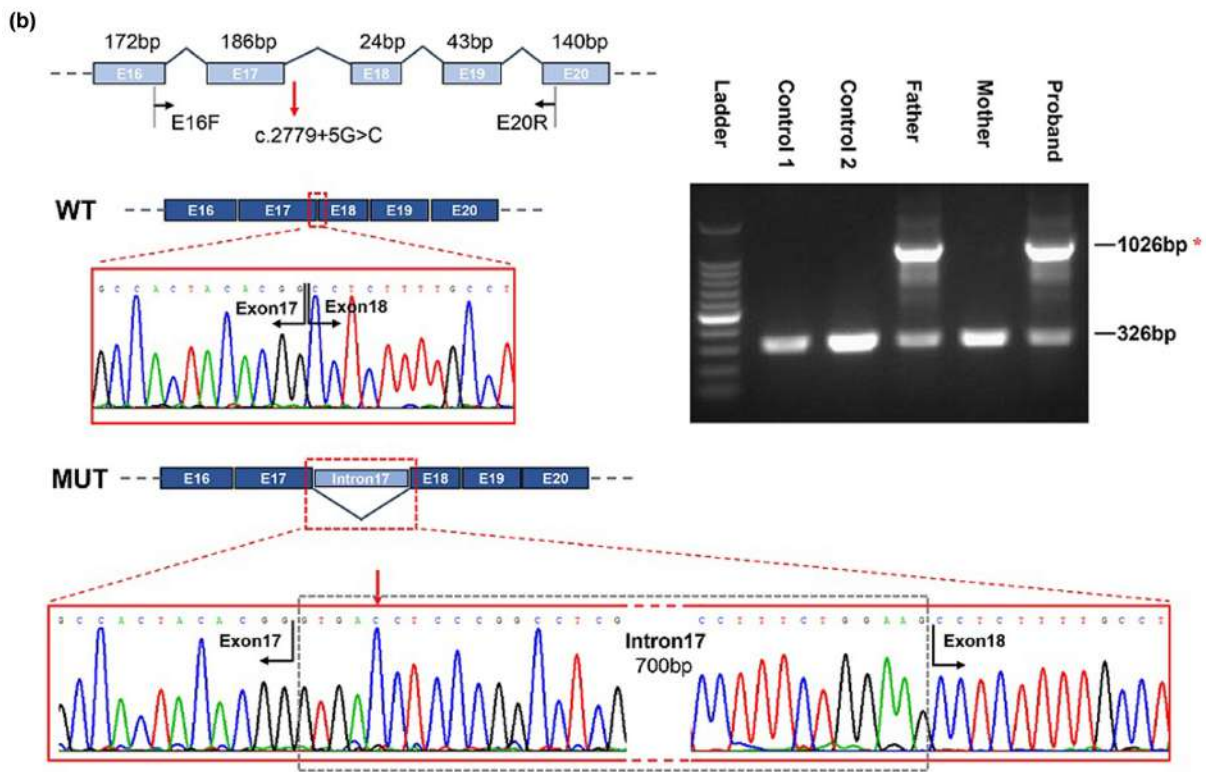
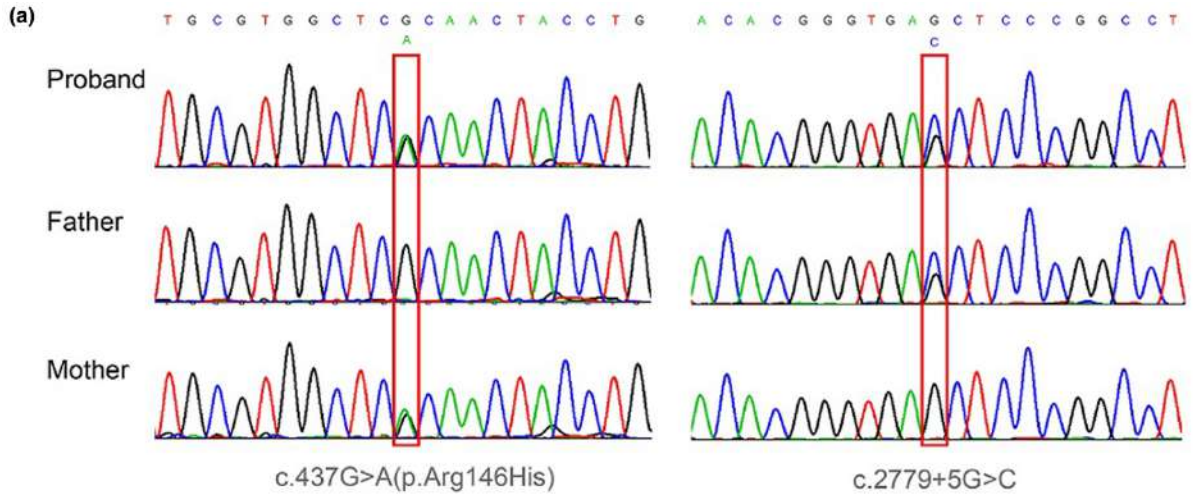


FIGURE 1 Pedigree and clinical features. (a) The family pedigree. Arrow indicates the proband. Unaffected parents are both carriers. The second symptomatic child was not genetically verified. (b) Eye motility in patient. The eyes are shown at upgaze (upper), in primary position (central), downgaze (lower), left gaze (left), and at right gaze (right). (c) Thoracic and lumbar spine X-ray showing severe thoracic scoliosis with convexity to the right. (d) Severe scoliosis of the patient at the age of 16 years old.



(c)

Human	P R I V H G R R A R P D E G V Y T C V A R N Y L G A A A S R N A S L E V A V
Chimp	P R I V H G R R A R P D E G V Y T C V A R N Y L G A A A S R N A S L E V A V
Rhesus	P R I V H G R R A R P D E G V Y T C V A R N Y L G A A A S R N A S L E V A V
Mouse	P R I V H G R R S R P D E G V Y T C V A R N Y L G A A A S R N A S L E V A V
Rat	P R I V H G R R S R P D E G V Y T C V A R N Y L G A A A S R N A S L E V A V
Rabbit	P R I V H G R R A R P D E G V Y T C V A R N Y L G A A A S R N A S L E V A V
Pig	P R I V H G R R A R P D E G V Y T C V A R N Y L G A A A S R N A S L E V A V
Cow	P R I V H G R R A R P D E G V Y T C V A R N Y L G A A A S R N A S L E V A V
Horse	P R I V H G R R A R P D E G V Y T C V A R N Y L G A A A S R N A S L E V A V
Dog	P R I V H G R R A R P D E G V Y T C V A R N Y L G A A A S R N A S L E V A V
Elephant	P R I V H G R R A R P D E G V Y T C V A R N Y L G A A A S R N A S L E V A V
Chicken	L R I V H G R R S K P D E G I Y V C V A R N Y L G E A T S R N A S L E V A V
Z.tropicalis	L R I V H G R R S K P D E G V Y I C V A R N Y L G E S V S R N A S L E V A I
Zebrafish	L R I V H G R R S K P D E G V Y V C V A R N Y L G E A V S R N A S L E V A I

FIGURE 2 Genetic analysis results. (a) Variants identification by Sanger sequencing. The red frame represents the variant sites (c.437G>A and c.2779+5G>C, respectively). (b) Results of cDNA sequencing in the patient. (Top) Sketch map of cDNA sequencing in the study. The size of the exons is given above the drawing. The positions of the primers are noted below the physical map. (Right) RT-PCR products of *ROBO3* mRNA transcripts in the family separated on a 1.5% agarose gel. The aberrant mRNA fragment of 1026 bp is marked with a red asterisk. (WT, MUT) Sequencing results of cDNA. The corresponding physical maps are above the sequence diagram. Positions of displayed base sequence are noted by red dotted boxes. WT, wild-type sequence (326 bp); MUT, aberrant transcript with retention of 700 bp (gray dotted box). (c) Multispecies alignment of *ROBO3* protein. The red box represents the mutation site (Arg146). Multiple sequence alignments revealed that the Arg146 residue is highly conserved across mammalian species and some nonmammalian species.

4 | DISCUSSION

Here we reported a Chinese patient who had HGPPS and harbored compound heterozygous *ROBO3* mutations. The boy presented with congenital palsy of the horizontal gaze and early onset progressive scoliosis. He had a younger sister with similar symptoms. The reported median age for onset of scoliosis in patients with *ROBO3* mutations is 6 years (Chan et al., 2006; Fernández-Vega Cueto et al., 2016; Khan & Abu-Amero, 2014; Rousan et al., 2019; Volk et al., 2011; Xiu et al., 2021), but our patient developed scoliosis at an earlier age. In the vast majority of patients with HGPPS, horizontal gaze palsy appeared earlier than scoliosis, which was the case in our patient. However, patients with later-onset eye movement disorders have also been reported (Chan et al., 2006). In contrast to many other case reports, our patient did not present with nystagmus, and no other clinical symptoms associated with HGPPS, such as sensorineural hearing impairment, ipsilateral stroke, and nodding of the head, were observed (Amoiridis et al., 2006; Arlt et al., 2015; Bosley et al., 2005; Ng et al., 2011; Yamada et al., 2015). Approximately one-third of patients present with motor delay and several patients have shown intellectual disability (Xiu et al., 2021). Our patient did not significantly lag behind his peers in sitting unsupported but he did not start to walk independently until two and a half years of age. We suspected that this was associated with scoliosis, which may affect standing balance. Speech delay was also noted in our patient but significant cognitive deficits were not observed. This study emphasized that restricted ocular motility and progressive scoliosis were the core features of *ROBO3* mutations (Bosley et al., 2005; Jen et al., 2004).

Characteristic magnetic resonance imaging findings in the brainstem are exhibited in HGPPS patients. These include butterfly configuration of the medulla oblongata, hypoplastic split pons, and hypoplasia of the facial colliculi (Traboulsi, 2004). Despite our patient manifesting whit horizontal gaze palsy and scoliosis at an early stage, a clinical diagnosis had not been completed as the parents were reluctant for him to undergo a thorough physical examination. The patient received only routine eye examinations and a thoracic and lumbar spine X-ray. As there is no cure and medical treatment is limited for the

majority of genetic disorders, the patient had not received any relevant treatment. However, it has been reported that physical therapy can provide an effective intervention and can be used for the management of scoliosis (Farrar et al., 2017). A genetic test was not performed until the couple wanted a prenatal diagnosis to avoid the birth of an affected child.

The splice-site variant, c.2779+5G>C, is absent from the general population. It is not a canonical splicing variant and the PVS1 evidence code cannot be applied for the classification of the variant, in accordance with the ACMG/AMP guidelines. However, this substitution would decrease the acceptor site score (−95.23%) and may lead to exon skipping (Table S2), which has been predicted by the in silico varSeak website (<https://varseak.bio/>). To verify whether the variant affected mRNA splicing, we extracted mRNA from the leukocytes of the proband and his parents. Sanger sequencing of cDNA identified an aberrant transcript with intron retention (700 bp of intron 17), which contained a premature stop codon (c.2779+216_c.2779+218). Based on the experimental results, there was evidence that c.2779+5G>C warrants a PS3 variant designation and the transversion can be considered as likely pathogenic according to the ACMG/AMP variant classification (PS3 + PM2_supporting + PP4).

The missense variant, c.437G>A(p.Arg146His), was found in the gnomAD database but the alleles frequency was very low (MAF=0.00000455). The Arg146 residue is located in the first of five immunoglobulin (Ig)-like loops, which are implicated in a wide range of functions, such as cell–cell recognition, cell–surface receptors, muscle structure, and the immune system (Teichmann & Chothia, 2000). Multiple sequence alignments revealed that the Arg146 residue in *ROBO3* is a well-conserved amino acid among various species (Figure 2c). This variant is predicted to be pathogenic by multiple in silico programs (Table S2). Finally, this missense substitution is a likely pathogenic variant based on the following evidence: PM1 + PM2_supporting + PM3 + PP3 + PP4.

Although it may not provide a cure, molecular diagnosis of Mendelian diseases can improve disease management, offer prognostic information, and inform genetic counseling (Wang et al., 2018). With the rapid development of next-generation sequencing (NGS),

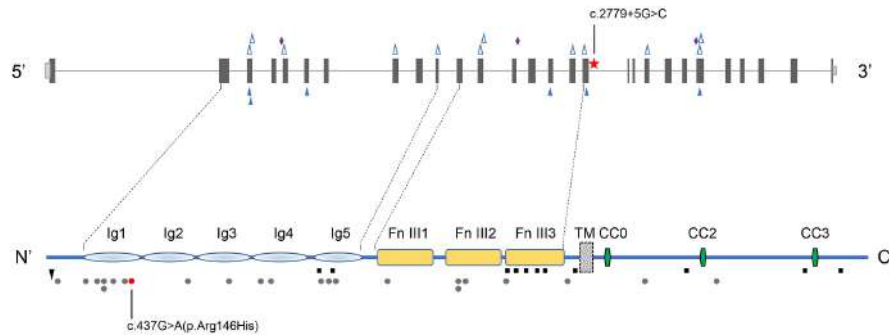


FIGURE 3 The spectrum of *ROBO3* mutations. The schematic presentation of the genomic structure of the *ROBO3* gene (upper) and the corresponding encoded protein domains (lower) are drawn in scale. Frameshift mutations are depicted by blue triangles (solid, insertion; hollow, deletion). Splicing mutations are marked with purple diamonds. The novel variant (c.2779+5G>C) is labeled with an asterisk. Nonsense mutations are represented by black squares. Missense mutations are indicated by gray dots. The missense variant in this paper (c.437G>A) is highlighted in red.

WES has become the most cost-effective manner for the analysis of monogenic disorders. For intronic substitutions outside the canonical ± 1 or 2 splice sites, minigene splicing reporter assays and effective mRNA analysis, using biological material from patients are important ways to confirm the effect on pre-mRNA splicing and to assess the pathogenicity of the variants. In this study, if the pathogenicity of the splice site transversion cannot be determined, the missense variation can only be assessed as a variant of unknown significance (VUS).

In order to survey the local mutation frequency in the *ROBO3* gene, we reviewed the in-house database ($n = 6886$) of previously identified *ROBO3* variants. After filtering out the common variants ($AF \geq 1\%$) and intronic variants, 121 variants, located in coding regions or splice sites, were selected for follow-up analysis. In accordance with the ACMG/AMP guidelines, 109 variants were classified as being of uncertain significance and eight variants were evaluated as likely pathogenic (7 novel and 1 reported), as shown in Table S3. In our cohort, the total AF was approximately 9.44×10^{-4} . In fact, the frequency may be higher, as some variants of unknown significance may eventually be reclassified as pathogenic variants. This result suggested that the *ROBO3* gene should be included in our local screening strategy (Guo & Gregg, 2019). We also speculated that some local patients with HGPPS have not been diagnosed due to the large population base in Guangxi.

5 | CONCLUSION

We described a boy with HGPPS and identified two novel mutations in the *ROBO3* gene. The patient displayed the core symptoms of HGPPS. We reported a novel substitution in a noncanonical splicing site of the *ROBO3* gene

that resulted in intron retention. In addition to these two mutations, we identified five novel variants that were likely pathogenic and we predicted the local AF of the *ROBO3* gene by reviewing our in-house database. The current findings will help to expand the mutation spectrum of the *ROBO3* gene (Figure 3) and indicate the importance of RNA sequencing for rare intronic variants that may affect splicing.

AUTHOR CONTRIBUTIONS

Collection of clinical data: Sheng Yi, Junjie Chen, and Jingsi Luo. Data analyzed and interpreted: Sheng Yi, Zailong Qin, Xunzhao Zhou, Shang Yi, Qiuli Chen, Limei Huang, and Qinle Zhang. Writing and review of the original draft of the manuscript: Sheng Yi, Biyan Chen, and Jingsi Luo.

ACKNOWLEDGMENTS

The authors appreciate the participating patients and their families.

FUNDING INFORMATION

This work is funded by the Guangxi Key Research and Development Program (GuikeAB17195004), the Health Department of Guangxi Zhuang Autonomous Region (No. Z20200678), and the Projects of Yu-Miao (grant no. GXWCH-YMJH-2017006). The funders had no role in study design, data collection and analysis, the decision to publish, or preparation of the manuscript.

CONFLICT OF INTEREST STATEMENT

The authors declare no conflict of interest.

DATA AVAILABILITY STATEMENT

The data sets generated and analyzed during the current study are available in the Sequence Read Archive (SRA) repository, NCBI, PRJNA852663.

ETHICS APPROVAL AND CONSENT TO PARTICIPATE

The study was approved by the ethics committee of the Maternal and Child Health Hospital of Guangxi Zhuang Autonomous Region. Written informed consent was obtained from parents or guardians of all patients.

ORCID

Sheng Yi  <https://orcid.org/0000-0002-2130-7701>

Zailong Qin  <https://orcid.org/0000-0001-7109-6693>

REFERENCES

- Amoiridis, G., Tzagnounissakis, M., Christodoulou, P., Karampekios, S., Latsoudis, H., Panou, T., Simos, P., & Plaitakis, A. (2006). Patients with horizontal gaze palsy and progressive scoliosis due to ROBO3 E319K mutation have both uncrossed and crossed central nervous system pathways and perform normally on neuropsychological testing. *Journal of Neurology, Neurosurgery, and Psychiatry*, *77*(9), 1047–1053. <https://doi.org/10.1136/jnnp.2006.088435>
- Arlt, E. M., Keindl, T. K., Grabner, G., Krall, E. M., & Meissnitzer, M. W. (2015). Horizontale Blickparese mit progredienter Skoliose [Horizontal gaze palsy with progressive scoliosis]. *Klinische Monatsblätter für Augenheilkunde*, *232*(3), 281–282. <https://doi.org/10.1055/s-0034-1396178>
- Bosley, T. M., Salih, M. A., Jen, J. C., Lin, D. D., Oystreck, D., Abu-Amero, K. K., MacDonald, D., al Zayed, Z., al Dhalaan, H., Kansu, T., Stigsby, B., & Baloh, R. W. (2005). Neurologic features of horizontal gaze palsy and progressive scoliosis with mutations in ROBO3. *Neurology*, *64*(7), 1196–1203. <https://doi.org/10.1212/01.WNL.0000156349.01765.2B>
- Chan, W. M., Traboulsi, E. I., Arthur, B., Friedman, N., Andrews, C., & Engle, E. C. (2006). Horizontal gaze palsy with progressive scoliosis can result from compound heterozygous mutations in ROBO3. *Journal of Medical Genetics*, *43*(3), e11. <https://doi.org/10.1136/jmg.2005.035436>
- Farrar, M. A., Park, S. B., Vucic, S., Carey, K. A., Turner, B. J., Gillingwater, T. H., Swoboda, K. J., & Kiernan, M. C. (2017). Emerging therapies and challenges in spinal muscular atrophy. *Annals of Neurology*, *81*(3), 355–368. <https://doi.org/10.1002/ana.24864>
- Fernández-Vega Cueto, A., Rodríguez-Ezcurra, J. J., & Rodríguez-Maiztegui, I. (2016). Horizontal gaze palsy and progressive scoliosis in a patient with congenital esotropia and inability to abduct. A case report. Parálisis de la mirada horizontal y escoliosis progresiva en un paciente con endotropia congénita y limitación de abducción. A propósito de un caso. *Archivos de la Sociedad Española de Oftalmología*, *91*(12), 592–595. <https://doi.org/10.1016/j.oftal.2016.05.002>
- Guo, M. H., & Gregg, A. R. (2019). Estimating yields of prenatal carrier screening and implications for design of expanded carrier screening panels. *Genetics in Medicine*, *21*(9), 1940–1947. <https://doi.org/10.1038/s41436-019-0472-7>
- Jen, J. C., Chan, W. M., Bosley, T. M., Wan, J., Carr, J. R., Rüb, U., Shattuck, D., Salamon, G., Kudo, L. C., Ou, J., Lin, D. D. M., Salih, M. A. M., Kansu, T., al Dhalaan, H., al Zayed, Z., MacDonald, D. B., Stigsby, B., Plaitakis, A., Dretakis, E. K., ... Engle, E. C. (2004). Mutations in a human ROBO gene disrupt hindbrain axon pathway crossing and morphogenesis. *Science*, *304*(5676), 1509–1513. <https://doi.org/10.1126/science.1096437>
- Khan, A. O., & Abu-Amero, K. (2014). Infantile esotropia with cross-fixation, inability to abduct, and underlying horizontal gaze palsy with progressive scoliosis. *Journal of AAPOS*, *18*(4), 389–391. <https://doi.org/10.1016/j.jaapos.2014.02.011>
- Ng, A. S., Sitoh, Y. Y., Zhao, Y., Teng, E. W., Tan, E. K., & Tan, L. C. (2011). Ipsilateral stroke in a patient with horizontal gaze palsy with progressive scoliosis and a subcortical infarct. *Stroke*, *42*(1), e1–e3. <https://doi.org/10.1161/STROKEAHA.110.591271>
- Richards, S., Aziz, N., Bale, S., Bick, D., das, S., Gastier-Foster, J., Grody, W. W., Hegde, M., Lyon, E., Spector, E., Voelkerding, K., Rehms, H. L., & ACMG Laboratory Quality Assurance Committee. (2015). Standards and guidelines for the interpretation of sequence variants: A joint consensus recommendation of the American College of Medical Genetics and Genomics and the Association for Molecular Pathology. *Genetics in Medicine*, *17*(5), 405–424. <https://doi.org/10.1038/gim.2015.30>
- Rousan, L. A., Qased, A. B. L., Audat, Z. A., Ababneh, L. T., & Jaradat, S. A. (2019). Horizontal gaze palsy and progressive scoliosis with two novel ROBO3 gene mutations in two Jordanian families. *Ophthalmic Genetics*, *40*(2), 150–156. <https://doi.org/10.1080/13816810.2019.1592199>
- Sharpe, J. A., Silversides, J. L., & Blair, R. D. (1975). Familial paralysis of horizontal gaze. Associated with pendular nystagmus, progressive scoliosis, and facial contraction with myokymia. *Neurology*, *25*(11), 1035–1040. <https://doi.org/10.1212/wnl.25.11.1035>
- Teichmann, S. A., & Chothia, C. (2000). Immunoglobulin superfamily proteins in *Caenorhabditis elegans*. *Journal of Molecular Biology*, *296*(5), 1367–1383. <https://doi.org/10.1006/jmbi.1999.3497>
- Traboulsi, E. I. (2004). Congenital abnormalities of cranial nerve development: Overview, molecular mechanisms, and further evidence of heterogeneity and complexity of syndromes with congenital limitation of eye movements. *Transactions of the American Ophthalmological Society*, *102*, 373–389.
- Volk, A. E., Carter, O., Fricke, J., Herkenrath, P., Poggenborg, J., Borck, G., Demant, A. W., Ivo, R., Eysel, P., Kubisch, C., & Neugebauer, A. (2011). Horizontal gaze palsy with progressive scoliosis: Three novel ROBO3 mutations and descriptions of the phenotypes of four patients. *Molecular Vision*, *17*, 1978–1986.
- Wang, J., Zhao, L., Wang, X., Chen, Y., Xu, M., Soens, Z. T., Ge, Z., Wang, P. R., Wang, F., & Chen, R. (2018). GRIPT: A novel case-control analysis method for mendelian disease gene discovery. *Genome Biology*, *19*(1), 203. <https://doi.org/10.1186/s13059-018-1579-x>
- Xiu, Y., Lv, Z., Wang, D., Chen, X., Huang, S., & Pan, M. (2021). Introducing and reviewing a novel mutation of ROBO3 in horizontal gaze palsy with progressive scoliosis from a Chinese family. *Journal of Molecular Neuroscience*, *71*(2), 293–301. <https://doi.org/10.1007/s12031-020-01650-4>
- Yamada, S., Okita, Y., Shofuda, T., Yoshioka, E., Nonaka, M., Mori, K., Nakajima, S., & Kanemura, Y. (2015). Ipsilateral

hemiparesis caused by putaminal hemorrhage in a patient with horizontal gaze palsy with progressive scoliosis: A case report. *BMC Neurology*, 15, 25. <https://doi.org/10.1186/s12883-015-0286-4>

SUPPORTING INFORMATION

Additional supporting information can be found online in the Supporting Information section at the end of this article.

How to cite this article: Yi, S., Qin, Z., Zhou, X., Chen, J., Yi, S., Chen, Q., Huang, L., Zhang, Q., Chen, B., & Luo, J. (2023). Early onset horizontal gaze palsy and progressive scoliosis due to a noncanonical splicing-site variant and a missense variant in the *ROBO3* gene. *Molecular Genetics & Genomic Medicine*, 11, e2215. <https://doi.org/10.1002/mgg3.2215>